ChemComm

Accepted Manuscript

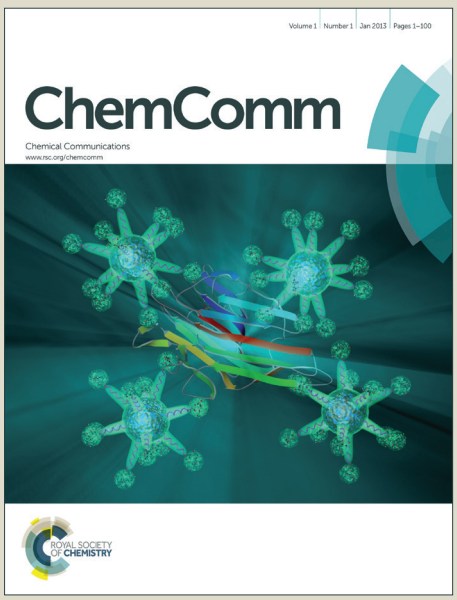

ROYAL SOCIETY OF CHEMISTRY

www.rsc.org/chemcomm

ChemComm

RSCPublishing

COMMUNICATION

Phase-transition contrast nanocapsule triggered by low-intensity ultrasound

Cite this: DOI: 10.1039/x0xx00000x

Hao Li,[a,b] Jianhao Wang,[a] Ping Wang,[c] Jian Zheng,[c] Fangfang Song,[d] Tinghui Yin,[c] Guofu Zhou,[b] Rongqing Zheng*[c] and Chao Zhang*[a]

Received 22th June 2014,
Accepted 25th Spetember 2014

DOI: 10.1039/x0xx00000x

www.rsc.org/chemcomm

A polymeric nanocapsule encapsulated with 1,1,1,3,3-pentafluorobutane was developed, in which 2,2,3,3,4,4,4-heptafluoro-1-butyl groups was introduced to the polymer terminal for high loading of liquid fluorocarbon. In vitro experiments demonstrate that its liquid/gas-phase transition can be triggered by mild heating. This nanocapsule can be harnessed as a contrast agent for tumor imaging under diagnostic ultrasound.

As the most widely used cost-effective diagnostic technique, ultrasonography lacks adequate precision and accuracy compared with other major medical imaging modalities.[1] Ultrasound contrast agents (UCA), represented by gas-filled microbubbles (usually with diameter of 1~7 μm), have served as echo-enhancers to increase the backscattering echo intensity in body fluid. The acoustic impedance, which is proportional to the echo intensity, can be greatly enhanced by the gas in the microbubbles that are usually intravenously administrated.[2] Hereinto, perfluorochemicals (PFC) is the most frequently used content in UCA owing to their strong hydrophobicity, low dispersity, and high biochemical stability.[1]

Although microbubbles have achieved amazing success in clinical practice, their applications in the imaging of capillary-abundant organs or tissues (e.g. tumor) are hindered mainly by their large size.[1] Nano-sized vehicles carrying gaseous or liquid PFCs have shown to be promising approaches to overcome such problems; however, the nanobubbles have rarely been investigated due to their high instability.[3] Nano-droplets of liquid PFCs, such as perfluorohexane (PFH; b.p. 58~60 ℃)[4,5] and perfluorooctyl bromide (b.p. 144 ℃)[6,7], have limitations on compressibility, *in vivo* persistency, structural stability[4,5,7], and much weaker imaging effects than microbubbles. Phase-change contrast agent (PCCA) based on thermally triggered phase-transition of encapsulated PFC [such as PFH and perfluoropentane (PFP; b.p. 29 ℃)], appears to be an attractive option for those applications.[8] Unfortunately, liquid-gas phase transition of PFH can be triggered by hyperthermia under the high intensity focused ultrasound (HIFU), but this operation is risky, invasive, and incapable of simultaneous imaging.[5] PFP-loaded nanoparticles would immediately transform into micron-sized bubble once injected into the body, due to its uncontrollable liquid/gas-phase transition under physiological conditions (~37 ℃).[9-15]

Therefore, 1,1,1,3,3-pentafluorobutane (PFB; b.p.: 40 ℃), which is structurally similar to PFC, is introduced as the inner droplet of nano-sized PCCA. Based on the higher temperature gradients of tumor region than surrounding normal tissue[16], PFB may readily undergo liquid/gas-phase transition with the aid of mild hyperthermia caused by low-intensity ultrasound (including clinical diagnostic ultrasound)[17]. PFB-loaded nanoparticles can be triggered to balloon till entering into tumor. Undoubtedly, this controllable transition of PFB under diagnostic ultrasound would avoid the uncontrollable liquid/gas-phase transition of PFP as well as the application of HIFU, thus could offer a safer and more convenient mode of imaging. Amphiphilic biodegradable block copolymer such as methoxy-poly(ethylene oxide)-b-poly(ε-caprolactone) (mPEG-PCL) has been used as the less gas-permeable "surfactant" to stabilize inner fluorocarbon droplet or bubble, to increase bubble resistance to pressure and to prolong blood circulation time.[1,10,12-14] Furthermore, according to previous reports[1,13,18], mPEG-PCL end-capped with 2,2,3,3,4,4,4-heptafluoro-1-butyl group (HFB) may have better compatibility with PFB and facilitate the formation of nano-sized polymeric PCCA.

In this paper, PFB nano-droplets were stabilized by HFB-terminated mPEG-PCL (mPEG-PCL-HFB) through an ultrasonic triple-emulsification process (Figure 1). In detail, liquid fluorocarbon (PFB or PFH) was first dispersed as droplets in dichloromethane (DCM), and then covered with copolymer chains to form aqueous emulsion under twice ultrasound action. After the removal of residual DCM, fluorocarbon-loaded polymeric nanocapsules with liquid core would be constructed in the stable form. This structure of these nanocapsules was confirmed by the transmission electron microscope (TEM) image of PFH-loaded mPEG-PCL-HFB nanocapsules (Figure 1). Uniform hollow spheres with diameter of about 600 nm could be observed with irregular loophole, which could be conceivably originated from the exhaustion of gasified PFH under high vacuum. Such observation clearly indicated that polymeric nanocapsule with the core of PFH was successfully constructed, and then cavitated by the gasification of PFH till burst. However, in the case of PFB, no such expansion or burst were observed under TEM; this could probably be attributed to the much higher volatility of PFB, which allows the droplet to evaporate too rapidly to generate the inner cavitation of the nanocapsules. Hereinto, mPEG-PCL and mPEG-PCL-HFB block copolymers with defined structure [molecular weight (M.W.) of PEG

block: 2,000 g/mol; M.W. of PCL block: 10,000 g/mol] were used. The particle sizing revealed that both copolymers could form nano-sized particles with the mean diameter ranging from 130 nm to 150 nm (Table 1). This size range would ensure the entry of these nanocapsules into tumor tissues through the gaps of vascular endothelium.[19] And according to the *Ideal Gas Law*, this size range would also ensure that most polymeric nanocapsules could expand to micron-scale upon the gasification of the encapsulated liquid fluorocarbon.

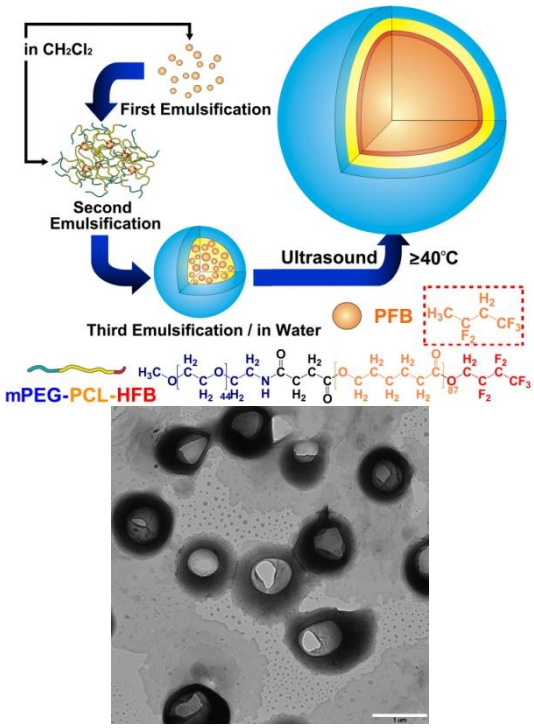

Figure 1. Schematic illustration of fabrication of polymeric nanocapsule loaded with liquid fluorocarbon (upper) and the TEM image (bottom) (Scale bar: 1 μm).

Table 1. Particle sizing and performance of PFH- or PFB-loaded nanocapsules.

Copolymer	Liquid Fluorocarbon	Particle Size (nm)*	Loading Efficiency %*	Encapsulation Efficiency %*
mPEG-PCL	PFH	135.1±44.4	41.8±1.2	4.3±0.2
	PFB	132.5±39.2	21.0±0.9	2.1±0.1
mPEG-PCL-HFB	PFH	148.0±46.0	71.0±0.9	14.7±0.6
	PFB	132.0±64.9	40.7±0.1	5.4±0.03

* average±STD, n≥3.

The key role of the HFB group was further verified through compatibility test. Figure 2A demonstrates that the terminal HFB group could obviously increase the static water contact angle of polymeric substrates, in the case of either block copolymers (mPEG-PCL and mPEG-PCL-HFB, respectively) or hydrophobic homopolymer blocks [benzyl-terminated PCL (Bz-PCL; M.W.: 10,000 g/mol) and 2,2,3,3,4,4,4-heptafluoro-1-butyl-terminated PCL (HFB-PCL; M.W.: 10,000 g/mol) respectively]. Particularly, the water contact angle of HFB-PCL (126.4 °) was much higher than the one of Bz-PCL (94.5 °), indicating that the presence of HFB group greatly improved the hydrophobicity of poly(ε-caprolactone) (PCL) blocks, which in turn would undoubtedly help strengthen their interaction with strongly hydrophobic fluorocarbon in the fabrication of nanocapsules. On the other hand, the interaction between HFB end group and fluorocarbon could also benefit the assembly of the block copolymers as evidenced by the thermal analysis of blank copolymers as well as the lyophilized nanocapsules (Figure 2B, 2C).

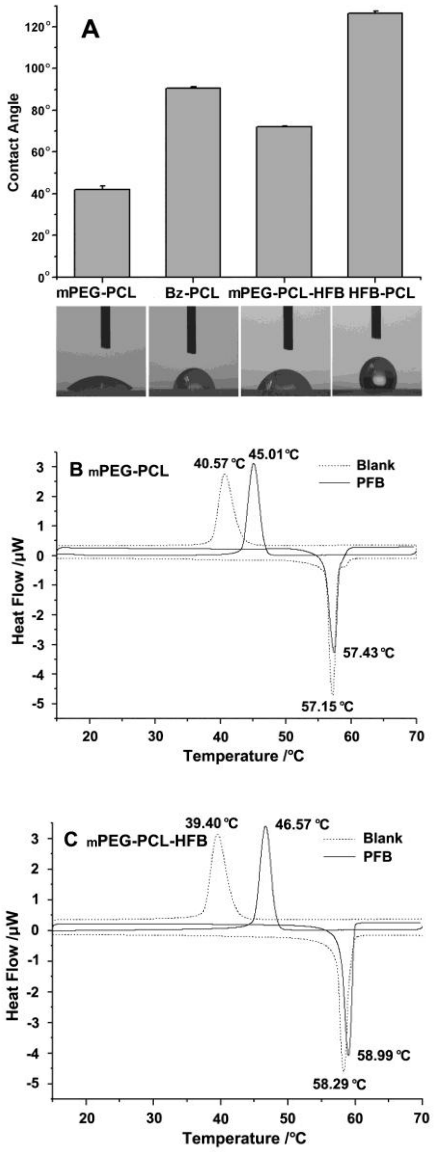

Figure 2. Compatibility tests of copolymers and PFB: the static water contact angle (A), the calorimetric curves of blank (B), and PFB-loaded nanocapsules (C).

Not surprisingly, the DSC curve of blank mPEG-PCL was quite similar to those in literatures, and that of blank mPEG-PCL-HFB displayed somewhat difference in cold crystallization temperatures (T_{cc}) and crystallinity[20, 21]. After encapsulation of fluorocarbon, the T_{cc} of lyophilized mPEG-PCL and mPEG-PCL-HFB nanocapsules increased from about 40 ℃ to above 45 ℃. Naturally, the hydrophobic interaction between PCL blocks and liquid fluorocarbon would help PCL blocks to form a well-organized hydrophobic layer on the surface of liquid fluorocarbon, which contributes to the enhanced crystallization of semicrystalline PCL blocks with higher T_{cc}. The presence of the HFB group would further reinforce this interaction and induce higher crystallinity of PCL blocks (Table 2); as a result, the mPEG-PCL-HFB

nanocapsules displayed higher crystallinity than its mPEG-PCL counterparts.[22] In addition, the loading capacity of liquid fluorocarbons in polymeric nanocapsules was also improved in the presence of HFB group as a result of the enhanced hydrophobic interaction between the copolymer and liquid fluorocarbon (Table 1). For example, the encapsulation efficiencies of PFH and PFB were more than doubled after the introduction of HFB to the block copolymer.

Table 2. Thermal properties of blank and PFB-loaded nanocapsules.

Sample ID		T_{cc} (℃)[a]	T_m (℃)[b]	ΔH_f (J/g)[b]	Crystallinity (%)[c]
mPEG-PCL	Blank	40.57	57.15	49.36	36.29
	PFB	45.01	57.43	53.25	39.15
mPEG-PCL-HFB	Blank	39.40	58.29	53.07	39.02
	PFB	46.57	58.99	61.62	45.31

a T_{cc}: cold crystallization temperature, second cooling, 1 ℃/min. b T_m: melting temperature, first heating, 1 ℃/min. c ΔH_f (heat of fusion) for 100% crystalline PCL: 136 J/g. [21]

The liquid-gas phase transition of fluorocarbon-loaded polymeric nanocapsules was visualized at determined temperature on a programmed heating stage under microscope (Figure 3). More visible micron-sized spherical bubbles appeared as the sample being heated from room temperature to the b.p. of fluorocarbon or higher temperature. Initially, very few microbubbles could be observed at 37 °C; more microbubbles were visible when the temperature was raised to slightly higher than boiling point of corresponding fluorocarbon, indicating the liquid-gas phase transition of fluorocarbon occurred inside the nanocapsule at elevated temperature. Quantification of microbubbles at determined temperature clearly indicated that the introduction of HFB group had significantly increased the number of microbubbles at elevated temperature. This could be explained by the higher encapsulation efficiency of liquid fluorocarbon as evidenced by chromatographical measurement (Table 1, and Figure S3 in ESI). Particularly, PFB-loaded nanocapsules generated much more microbubbles after grafting HFB groups to the mPEG-PCL copolymer as compared with their counterparts; at 41 ℃, the number of microbubbles significantly increased from 9 to 38. Those findings proved that these nanocapsules with liquid nanodroplets of PFB or PFH inside have the potential to generate micron-sized bubbles under mild heating. Since tumor tissue has higher acoustic impedance and slightly higher temperature compared with normal tissue, a temperature slightly higher than 40 °C can be readily achieved based on the mild hyperthermia effect under low intensity ultrasound. Thus the above PFB-loaded nanocapsules could be harnessed for *in vivo* imaging of tumor tissue under low intensity ultrasound such as diagnostic ultrasound.

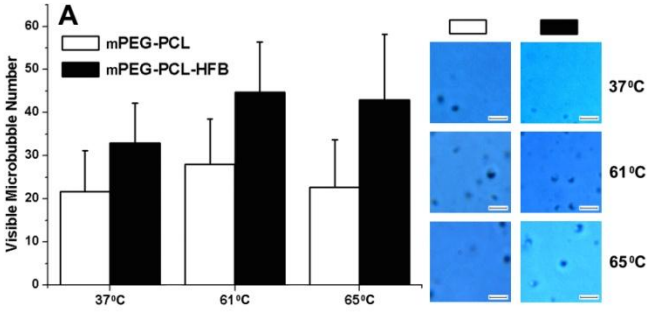

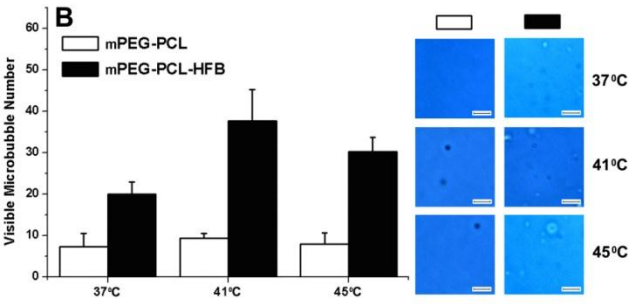

Figure 3. Visualization of the liquid-gas phase transition of polymeric nanocapsules loaded with PFH (A) and PFB (B) at different temperature under microscope. (Scale bar: 5μm)

In vitro ultrasound imaging test of these nanocapsules was performed utilizing an agarose model. PFB-loaded nanocapsules exhibited remarkably enhanced imaging at 40 ℃ where more off-white dots emerged compared with the initial stage (Figure 4A). After background subtraction, two times-diluted PFB-loaded mPEG-PCL-HFB nanocapsule (labelled mPEG-PCL-HFB-2X) exhibited enhanced gray values for about 30 second (s), and mean gray values were higher than background by at least 10 for about 17 s (Figure 4B). It proved that PFB-loaded mPEG-PCL-HFB nanocapsules could produce strong and long-lasting contrast. Since the UCA would be diluted in the circulation system after IV administration, difference dilutions of the nanocapsule solution were also test (Figure 4C) under same conditions. Clearly, 40 times-diluted nanocapsule solution still exhibited weakly enhanced imaging as compared with background, indicating the feasibility of intravascular and blood-pool imaging by intravenous injection (Figure 4D).

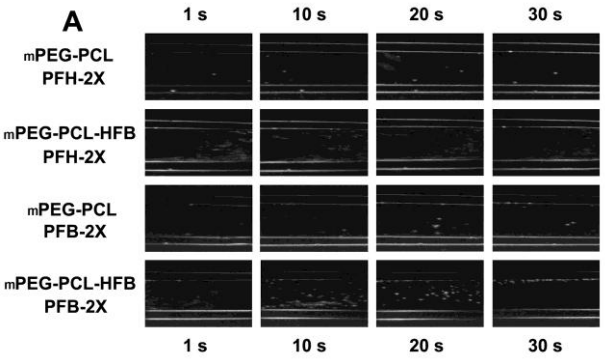

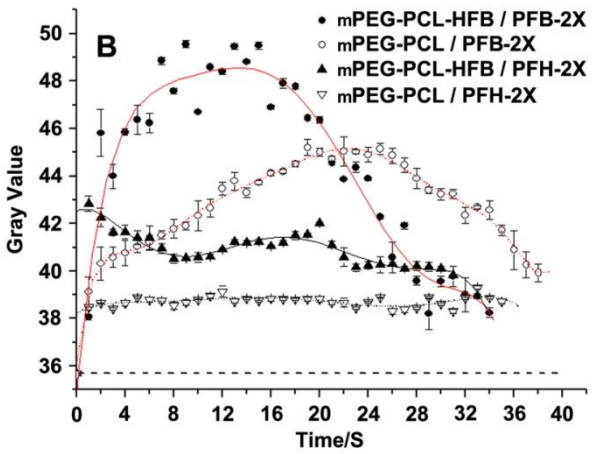

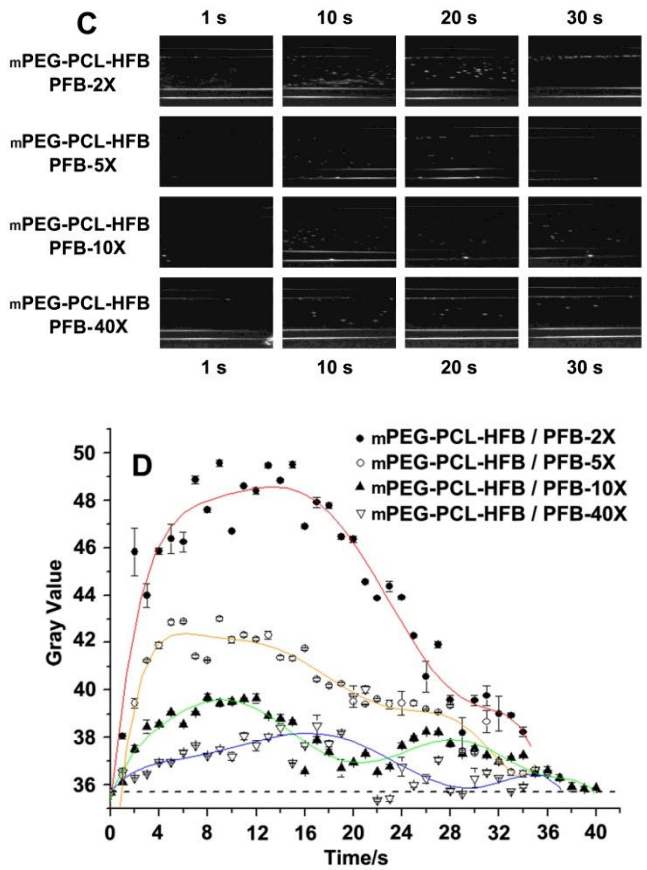

Figure 4. *In vitro* ultrasound imaging and gray value of solutions of liquid PFB- or PFH-loaded nanocapsules (A and B), and the PFB-loaded nanocapsules at different dilution ratio (C and D).

Conclusions

Liquid fluorocarbon-encapsulated polymeric nanocapsules were constructed, in which the HFB groups in the block copolymer could greatly enhance the loading capacity of liquid fluorocarbon. In vitro ultrasound imaging demonstrated that the liquid/gas-phase transition and resulting imaging of nanocapsules could be triggered by mild heating. This novel approach has paved the way for accurate imaging within tumor region *via* mild hyperthermia of diagnostic ultrasound. More efforts on the improvement in expansion ratio, optimization of nanocapsule concentration, and even introduction of targeting ligands for tumor-specific ultrasound molecular imaging would be the focus of the future study.

The authors thank Mr. Yihan Jing for his assitance in microscopic observation. This work was supported by National Natural Science Foundation of China (21004080, 51203195 and 81271577), and the Program for New Century Excellent Talents in University of the Ministry of Education of China (NCET-09-0818).

Notes and references

[a] *School of Engineering, Sun Yat-Sen University, Guangzhou 510006, P. R. China. Fax: +86 20 3933 2312; Tel: +86 20 3933 2145; E-mail: zhchao9@mail.sysu.edu.cn*

[b] *Institute of Electronic Paper Display, South China Academy of Advanced Optoelectronics, South China Normal University, Guangzhou 510006, P. R. China.*

[c] *Department of Ultrasonography, The Third Affiliated Hospital, Sun Yat-Sen University, Guangzhou 510630, P. R. China. Fax: +86 20 8573 6401; Tel: +86 20 8551 6867-3030; E-mail: zhengrongqin@hotmail.com*

[d] *School of Chemistry and Molecular Sciences, Wuhan University, Wuhan 430072, P. R. China.*

Electronic Supplementary Information (ESI) available: [Materials, synthesis, and characterizations]. See DOI: 10.1039/c000000x/

1 E. G. Schutt, D. H. Klein, R. M. Mattrey and J. G. Riess, *Angew. Chem. Int. Ed.*, 2003, **42**, 3218.
2 F. Calliada, R. Campani, O. Bottinelli, A. Bozzini and M. G. Sommaruga, *European Journal of Radiology*, 1998, **27**, S157.
3 Y. Wang, X. Li, Y. Zhou, P. Huang and Y. Xu, *International Journal of Pharmaceutics*, 2010, **384**, 148.
4 M. Chang, E. Stride and M. Edirisinghe, *Soft Matter*, 2009, **5**, 5029.
5 X. Wang, H. Chen, Y. Chen, M. Ma, K. Zhang, F. Li, Y. Zheng, D. Zeng, Q. Wang and J. Shi, *Adv. Mater.*, 2012, **24**, 785.
6 E. Pisani, N. Tsapis, B. Galaz, M. Santin, R. Berti, N. Taulier, E. Kurtisovski, O. Lucidarme, M. Ourevitch, B. T. Doan, J. C. Beloeil, B. Gillet, W. Urbach, S. L. Bridal and E. Fattal, *Adv. Funct. Mater.*, 2008, **18**, 2963.
7 R. D íz-L ópez, N. Tsapis, M. Santin, S. L. Bridal, V. Nicolas, D. Jaillard, D. Libong, P. Chaminade, V. Marsaud, C. Vauthier and E. Fattal, *Biomaterials*, 2010, **31**, 1723.
8 P. S. Sheeran and P. A. Dayton, *Current Pharmaceutical Design*, 2012, **18**, 2152.
9 J. M. Correas, and S. D. Quay, *Clinical radiology*, 1996, **51**, 11.
10 Z. Gao, A. M. Kennedy, D. A. Christensen and N. Y. Rapoport, *Ultrasonics*, 2008, **48**, 260.
11 Y. T. Lim, Y. Noh, J. Cho, J. H. Han, B. S. Choi, J. Kwon, K. S. Hong, A. Gokarna, Y. Cho and B. H. Chung, *J. Am. Chem. Soc.*, 2009, **131**, 17145.
12 N. Y. Rapoport, A. M. Kennedy, J. E. Shea, C. L. Scaife and K. Nam, *Journal of Controlled Release*, 2009, **138**, 268; N. Rapoport, A. M. Kennedy, J. E. Shea, C. L. Scaife and K. Nam, *Molecular Pharmaceutics*, 2010, **7**, 22.
13 K. Shiraishi, R. Endoh, H. Furuhata, M. Nishihara, R. Suzuki, K. Maruyama, Y. Oda, J. Jo, Y. Tabata, J. Yamamoto and M. Yokoyama, *International Journal of Pharmaceutics*, 2011, **421**, 379.
14 N. Rapoport, K. Nam, R. Gupta, Z. Gao, P. Mohan, A. Payne, N. Todd, X. Liu, T. Kim, J. Shea, C. Scaife, D. L. Parker, E. Jeong and A. M. Kennedy, *Journal of Controlled Release*, 2011, **153**, 4.
15 C. Wang, S. Kang, Y. Lee, Y. Luo, Y. Huang and C. Yeh, *Biomaterials*, 2012, **33**, 1939; A. Liberman, H. P. Martinez, C. N. Ta, C. V. Barback, R. F. Mattrey, Y. Kono, S. L. Blair, W. C. Trogler, A. C. Kummel and Z. Wu, *Biomaterials*, 2012, **33**, 5124; K. Wilson, K. Homan1 and S. Emelianov, *Nature Communications*, 2012, **3**, 1.
16 R. Lawson, *Canadian Medical Association Journal*, 1956, **75**, 309; P. Carmeliet and R. K. Jain, *Nature*, 2000, **407**, 249.
17 S. Mitragotri, *Nautre Reviews*, 2005, **4**, 255.
18 M. L. Fabiilli, J. A. Lee, O. D. Kripfgans, P. L. Carson, and J. B. Fowlkes, *Pharm. Res.*, 2010, **27**, 2753.
19 S. K. Hobbs, W. L. Monsky, F. Yuan, W. G. Roberts, L. Griffith, V. P. Torchilin, and R. K. Jain, *Proc. Natl. Acad. Sci. USA*, 1998, **95**, 4607.
20 B. Bogdanov, A. Vidts and E. Schacht, *Macromolecules*, 1999, **32**, 726.
21 C. He, J. Sun, T. Zhao, Z. Hong, X. Zhuang, X. Chen and X. Jin, *Biomacromolecules*, 2006, **7**, 252.
22 B. Chen and J. R. G. Evans, *Macromolecules*, 2006, **39**, 747.

